The effect of temperature on the critical electric field for electroporation: A single cell electroporation device study

DIAZ-RIVERA RUBENE[1*], RUBINSKY BORIS[2]

[1] *Department of Mechanical Engineering, University of Puerto Rico at Mayagüez, PR 00681 Puerto Rico and*
Weldon School of Biomedical Engineering, Purdue University;<rubene.diaz@upr.edu>
[2] *Department of Mechanical Engineering, University of California, Berkeley, Berkeley, CA 94720, USA <rubinsky@berkeley.edu>*

Abstract: Electroporation is the permeabilization of the cell membrane with brief, high electric fields. It is a technology of importance in bioengineering and medicine. An experimental study was performed to determine the effect of temperature on the electroporation parameters in individual cells. For this purpose, we designed a microelectromechanical device that maintains a controlled temperature and detects the threshold of electroporation by incorporating an individual cell into an electronic circuit. A series of experiments were performed with Madin-Darby Canine Kidney (MDCK) cells. We have found that the electrical field corresponding to the onset of electroporation, known as the critical electric field (E_C), is a strong function of temperature. It increases with decreasing temperature. The critical electric field for electroporation at 5°C is as much as two times that needed to electroporate the cells at 37°C.

1. Introduction

The cell membrane is a structure consisting mainly of lipid molecules and proteins. They are arranged in a fluid mosaic, that provides highly selective permeability properties. This selectivity of the cell membrane to different types of molecules plays a fundamental role in cell physiology. In many medical and

---

*Correspondence address: rubene.diaz@upr.edu

biotechnology applications, it is important to transfer chemical species for which the membrane is impermeable, across the cell membrane. Over the past few decades, different techniques have been developed to overcome the biological barrier of the cell membrane in a controlled way. Some of the mechanisms employed by these techniques bypass the cell membrane barrier by chemical, electrical or mechanical means. In this report, membrane permeabilization by electrical means is explored. The technique that employs this mechanism is known as electropermeabilization, or electroporation. Electroporation involves the application of a high intensity electric field pulse (~1kV/cm) of short duration (~10^{-6} to 10^{-1} sec) to cells and/or tissues, which causes a dramatic increase of the membrane permeability [1, 2]. According to experimental observations, it is believed that during electroporation there is a rapid localized structural rearrangement within the membrane, which creates water-filled pores [3, 4]. These aqueous pathways, or hydrophilic pores, transverse the membrane and tremendously increases the ionic and molecular transport through it [5, 6].

Electrical pulses can, as a function of pulse amplitude, shape or duration, have either no effect on the cell membrane or induce permeabilization in a reversible or irreversible fashion. Reversible permeabilization refers to the process of the electropore resealing in the membrane after the application of the electric pulse whereas in irreversible electroporation, the membrane remains permeable and the cell dies. Probably the most important electrical pulse regime for medicine and biotechnology is that which induces reversible electroporation. However, the reversible permeabilizing effects of electrical fields occur in a very narrow range of electrical parameters. For practical use of electroporation, it is particularly important to determine the electrical parameters that distinguish between the conditions of no electroporation to the onset of reversible electroporation, i.e. the "critical electric field, E_C" for the onset of electroporation. Currently these parameters are determined through trial and error mass transfer experiments, which involve the transfer of marker molecules across the cell membrane and detection of these molecules, or their effect on the cell. Current studies employ batches of very large number of cells and the data is averaged.

A fundamental understanding of the biophysical processes, which occur during the application of an electrical field across a single cell, could facilitate the optimal use of electroporation. Studies show that the process of electroporation is related to the properties of the cell membrane. The electrical and mechanical properties of the cell membrane can become affected by changes in temperature [7-10]. The goal of this study is to investigate the effects of temperature on the relation between electrical parameters and the electroporation process and in particular on the value of the critical electric field. To this end, a new device was developed, which was built with micro-electromechanical (MEMS) technology. This device has the ability to determine the permeability properties of the cell membrane as a function of temperature and electrical parameters, in individual cells. To the best of

our knowledge this is the first archival scientific report on the effects of temperature on the critical electric field for electroporation in single cells.

Earlier studies on the effect of temperature on electroporation showed contradictory findings. In the late 70's, Zimmermann and his group studied the effect of temperature on the membrane breakdown for artificial lipid bilayers and algae cells [11, 12]. They found a strong temperature dependence on the critical electric field for membrane breakdown in both artificial and natural cell membranes (i.e., an increase by a factor of 2 with decreasing temperature from 30 to 4°C for oxidized cholesterol/n-decane lipid bilayers and algae cells, *Valonia utricularis*). However, there are other reports that show little temperature dependence on the critical voltage for human erythrocytes, demonstrating that this behavior is dependent on the membrane constituents as well [13]. Recent studies have also shown the relationship between temperature and the critical electric field for electroporation in skin [14, 15]. Nevertheless, the overall trend of the critical voltage is to increase as the membrane temperature decreased. In general, there is no thorough understanding of the fundamental mechanism of electroporation and its relationship with temperature. Furthermore, all the previous studies were done on batches of cells. Our objective is to provide additional experimental information on the effect of temperature on the electroporation threshold in individual cells to further expand the understanding of the process of electroporation.

As part of a comprehensive study on the effects of temperature on the electroporation of single cells, a micron scale device capable of integrating a single cell into an electronic circuit was designed. The system, which is conceptually similar to a device previously developed by our group [16, 17], allows us to probe the cell's membrane permeability to ions. The device consists of dielectric thin film sandwiched between two Ag/AgCl electrodes. A microhole in the middle of the dielectric film opens an ionic pathway between two chambers formed by the electrodes and the dielectric film. The micro aperture is used to capture single cells by means of a pressure differential. When the electrical field is applied, the current travels through the microhole, and, around or through the trapped cell. Real time measurements of the voltage and the ionic current provide us with real time information as to when the membrane ionic barrier has been compromised. With this technique, we studied the effects of temperature on cell membrane permeabilization with controlled electrical fields delivered across individual cells. A strong dependence on temperature was observed and an explanation is proposed.

2. Materials and Methods

2.1. Microhole chip fabrication and systems set-up

The system is based on a dielectric membrane formed from a single crystal silicon (SCS) chip with a deposited thin film of low stress silicon nitride (LSN), two chambers, two electrodes and one microhole. Silicon nitride was chosen as the

passivation layer because it is a good mask material for typical silicon etchants and is translucent to visible light in the thin film regime. This enabled the incorporation of conventional microscopic techniques to our system.
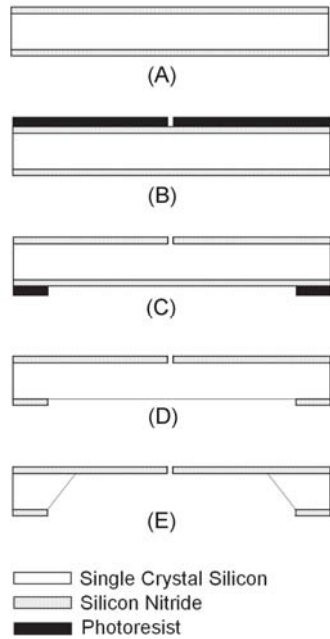
Fig. 1. Cross section of the fabrication process for the micro opening
on the silicon substrate.

Fig. 1 shows the step-by-step fabrication process for the central component, the dielectric membrane. The process begins with a ⟨100⟩ n-type, double side polished, single crystal silicon (SCS) wafer. Low Pressure Chemical Vapor Deposition was used to deposit a 1µm, low stress, silicon nitride layer on each side of the wafer (Fig. 1A). Photoresist was spun on the top of the wafer and the microhole was patterned with a photolithography contact printer (Fig. 1B). The patterned microhole was etched through the silicon nitride film using plasma etching. Typical diameters of the microhole range from 3 to 6 µm in different devices that were fabricated. After stripping off the photoresist left on the top of the wafer, a new layer of photoresist was deposited and patterned on the backside of the wafer to open a window for the KOH etch step (Fig. 1C). Then, the back window was opened with plasma etching (Fig. 1D). Once the microhole and the back window were patterned on the silicon nitride layer, the wafers were dipped into a KOH solution (H2O: KOH = 2:1 by weight) at 80°C to etch the exposed SCS all the way (Fig. 1E). Finally, a 0.1 µm silicon dioxide isolation layer was thermally grown over the exposed SCS after the KOH etch (not shown).
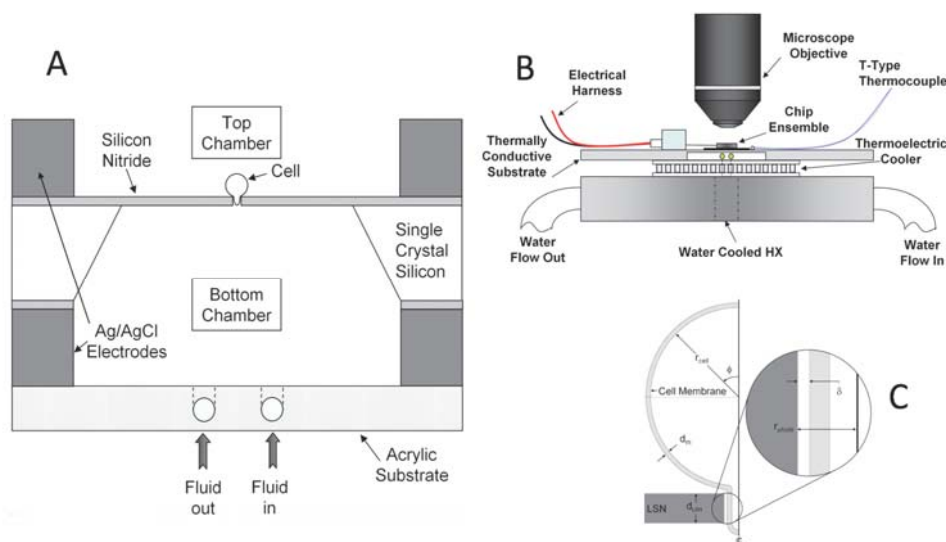
Fig. 2. A) Graphical representation of the microhole chip ensemble cross section. B) Side view of the chip ensemble coupled with the temperature controlled stage (not to scale). C) Schematic of the way in which a cell is captured in the microhole.

A cross section of the microhole chip ensemble is shown in Figure 2 A. The top and the bottom chambers were created by bonding two annular Ag/AgCl electrodes to the chip (In Vivo Metric, Healdsburg, CA). The electrodes were then mounted on an epoxy housing (Henkel Loctite Corp., Rocky Hill, CT). Finally, the bottom chamber was sealed by bonding the bottom electrode to an acrylic substrate. The acrylic substrate contained inlet and outlet fluid ports that were used to control the pressure in the system.

Temperature was controlled by mounting the chip ensemble into a thermally conductive substrate attached to a thermoelectric cooler (see Fig. 2B, Melcor Corp., Trenton, NJ). Since the thermoelectric cooler (TEC) only moves the heat from one side to the other, there is a need to dissipate the heat from the hot junction. To remove the heat from the TEC, a water-cooled heat exchanger was fabricated. The heat exchanger consists in a disk shaped aluminum piece with an annular cavity inside. The water flows from one side of the heat exchanger to the other removing the heat from the Peltier effect device. The hole in the heat exchanger facilitated the use of transmitted light microscopy for the experiments.

To minimize contact resistance among the thermally conductive surfaces, a silver-based thermal compound was used (Arctic Silver Inc., Visalia, CA). The TEC was connected to a DC power supply through a solid state relay. The solid state relay was turned on or off by a PID temperature controller depending on the set point and the temperature feedback (Fuji Electric Corp., Saddle Brook, NJ). A T-type thermocouple was used to measure the temperature (Therm-x of California, Hayward, CA).

A schematic of the way in which part of the cell is trapped in the microhole by means of a pressure differential between the top and bottom chambers is shown in Fig. 2C.

2.2. Cells used in study

Madin-Darby Canine Kidney (MDCK) epithelial cells were grown in Dulbecco's Minimum Essential Medium (Invitrogen Corp., Carlsbad, CA), Earle's balanced salt solution supplemented with 10% fetal bovine serum, 1% non-essential amino acids, 1% penicillin, and 2 mM of L-glutamine. The temperature inside the incubator was maintained at 37°C with a constant supply of medical grade air mixture at 5% CO_2. For electroporation experiments, the culture medium was replaced by Dulbecco's PBS (136mM NaCl, 8mM Na_2HPO_4, 2.7 mM KCl, 1.5 mM KH_2PO_4). The cells where removed from the culture flask by using 0.25% Trypsin/EDTA. Two PBS washes were performed prior to the addition of trypsin/EDTA.

2.3. Experimental procedure

In a typical experiment, both chambers were filled with a physiological phosphate buffer saline (PBS) and MDCK cells were introduced into the top chamber via micropipette. A negative pressure was applied to the system by controlling the fluid ports. The low-pressure zone pulled the closest cell into the microhole in a matter of seconds and effectively plugged the microhole, as shown in Fig. 2C. An Olympus BX-60 upright microscope was used to monitor the cell trapping procedure (Olympus America Inc., Melville, NY).

When a DC voltage potential is applied across the system, the ionic current is forced through the seal between the hole and the cell (when the cell membrane integrity is not breached and there is no electroporation) or through both the seal and the cell membrane (if the electric field is high enough to induce electroporation). The current through the system is measured *in vitro,* thereby providing us with real time information of the permeability state of the cell membrane.

The size of the microhole used for experimentation was 3 ± 0.1 μm in diameter. The temperature was varied from 37 to 5°C in intervals of 5 degrees and the pressure applied to trap every cell was - 2.0 ± 0.1 kPa. Excellin Life Sciences Inc. (Berkeley, CA) provided the electronics and the software. The details on the electronics can be found elsewhere [18]. A National Instruments Data Acquisition Card was used to transmit the data from the electronics box to a personal computer (National Instruments Corp., Austin, TX).

To study electroporation, a triangular voltage waveform was used as an input to the system. The triangular waveform was chosen because we could get a specific

value for the voltage needed to induce electroporation by measuring the real time change in the current. The ramping rates used for the experiments reported in this study are 5 Volts per second. The maximum voltage was set to 1 V; therefore, the ramping rate adjusts the time length of the pulse. In each experiment, the voltage and the current were measured simultaneously. Direct current recordings were performed while the biological cells were trapped in the microhole. Eight cells were electrically probed at each temperature and ramping rate for a total of 168 electrical recordings.

For each experiment, one 100 mV squared non-electroporation pulse was applied to the cell before the main pulse (triangular waveform), to measure the system electrical resistance. The amplitude of the pre-pulse is far below the voltage needed to induce electroporation at any probed temperature. The purpose of this initial measurement was to confirm that the cell was captured in the microhole.

2.4. Electrical model

To analyze the electric field driven processes that the cells experience during the experiments, we developed an equivalent electrical circuit of the system. Figure 3A shows the part of the cell entrapped in the hole prior to the delivery of the electroporation pulse, and the path of ion flow during the application of the pulse. Figure 3B shows the path of ionic flow after the cell membrane has become electroporated. Before electroporation, the cell membrane capacitance is the dominant electrical component. After electroporation, the cell membrane is impaired and there is an ionic flow through the cell. The corresponding lumped electrical circuits to Figs. 3A and 3B are Figs. 3C and 3D, respectively. Fig. 3C shows an equivalent electrical circuit of the cell trapped in the microhole where R_{seal} is the ionic resistance due to the presence of the phosphate buffer solution in between the cell membrane and the walls of the hole (seal resistance), R_{cyto} is the cytosol resistance and R_m and C_m are the cell membrane resistance and capacitance, respectively. The capacitance of the dielectric silicon nitrate layer is marked as C_{lsn}. Fig. 3D shows the equivalent electrical circuit after pores have formed in the electroporated cell membrane. The permeabilized membrane is considered as an open circuit. The composite resistance dominates the current flow and it can be assumed that the effect of capacitance in the system is negligible. Notice that R_{cell} is equivalent to the summation of R_m and R_{cyto}.

The equivalent resistance through the circuit, which is approximately the experimental resistance of the system, is given by the following equation.

$$R_{Eq.} = \frac{R_{seal}\ R_{cell}}{R_{seal} + R_{cell}} \tag{1}$$

Notice that we have omitted the resistance of the ionic solution in the top and bottom chamber for the development of the equivalent electrical circuit model. The omission comes from the fact that the cell and seal electrical resistances are

dominant in the system, thus the electrical resistance in both chambers becomes negligible.
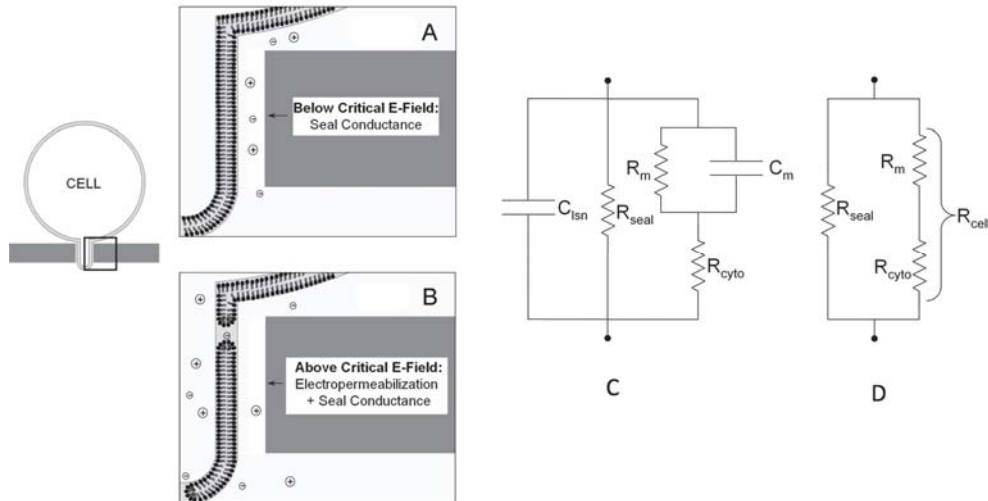
Fig. 3. Visual representation of the ionic flow in the system with a cell trapped in the microhole. Inset (A) shows the cell membrane exposed to an electric field below critical conditions. Here, the ions flow in between the cell membrane and the microhole wall (seal cleft conductance). Inset (B) shows the cell membrane exposed to an electric field above critical conditions (electropermeabilization). Here, the electroporated membrane provides an additional ionic pathway. C) Electrical schematic model of the microelectroporation system prior to electroporation. D) Electrical schematic model of the microelectroporation system after electroporation.

3. Results

3.1. Seal resistance

A typical resistance measurement for a cell trapped in the microhole when excited by a non-electroporation square pulse of 100 mV is shown in Fig. 4A. The resistance was calculated by dividing the overall imposed voltage by measured current.   Notice that the seal resistance found in Fig. 4A is on the order of magnitude of Mega Ohm, which is typical for planar microhole structure systems [18, 19]. In addition, notice that the resistance is constant over the time the system was excited. This means that the integrity of the cell membrane is intact with respect to the applied electric field and the measurement corresponds to the ionic solution found in between the envelope of the cell membrane and the wall of the micro aperture. This measurement is known as the seal resistance. The seal resistance is dependent on the distance between the cell membrane envelope that is embedded in the microhole and the wall of the microhole (see Fig. 3 A). The temperature dependence of the seal resistance and the biophysical configuration leading to this resistance have been previously characterized by us in [20].
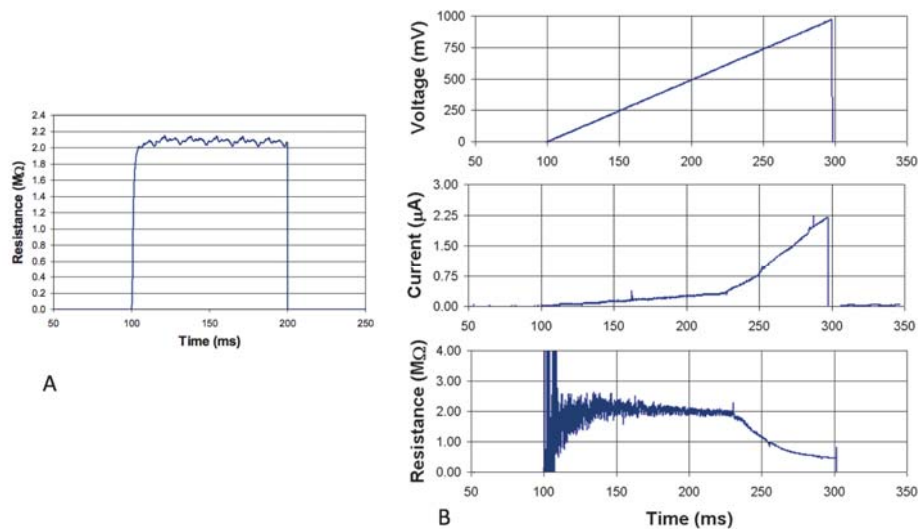
Fig. 4. A) Typical resistance of the system with a cell trapped in the hole for a 100 mV square pulse at 20°C. Notice that the resistance is constant throughout the pulse. This implies that electroporation has not occurred. B) Typical electrical recordings for the micro-electroporation chip with a cell trapped in the hole. The ramp rate for the illustrated triangular waveform is 5 V/s. The data was recorded at 20°C.

3.2. Critical voltage (V_C) at the onset of electroporation, as a measure of the critical electric field (E_C)

Fig. 4B, illustrates typical electrical recordings for the system with a cell in the microhole. Typical electrical data includes measured voltage and current and computed resistance. To generate the data in Fig 4B, the applied voltage was ramped from 0 to 1 volt in 200 milliseconds (a ramp rate of five Volts per second). A closer examination of Fig 4B, reveals a non-linear behavior of the current readings as the voltage is increased from 0 to 1 volt. The current increases linearly with the voltage for the first 130 milliseconds, when the current slope changes abruptly. The sudden change in slope indicates that electropermeabilization has occurred. It is clear from Fig. 4B that the current curve can be separated into two segments, which represent different ionic pathways. The first segment represents the behavior of the system below critical electric field conditions. Here, the major ionic pathway is between the outer surface of the cell membrane and the wall of the microhole, assuming very low membrane conductance (this is known as the seal cleft conductance, see Figs. 3A and 3C). The second segment represents the behavior of the system above critical electric field conditions, where the electropermeabilized membrane provides an extra current pathway, Figs. 3B and 3D. The applied potential at the point where the two segments of the current curve meet corresponds to the conditions at the onset of electroporation. This study deals with the effect of temperature on the onset of electroporation. Because all the

design parameters remain the same, in all the experiments, we will use, from now on, the voltage measured at the point of intersection of the two current segments as a measure for the critical electric field (E_C). The critical voltage (V_C) measured at the onset of electroporation, should be regarded as a surrogate for E_C. V_C was calculated by curve fitting the current data for each experiment before and after the change in slope, then solving for the voltage at the intersection of the lines. Because V_C, represents the real measured data, we will discuss the effects of temperature on electroporation in terms of this variable.

Figure 5, shows a graph of the raw data, depicting the measured current for every input voltage, at each studied temperature for the ramp rate of 5 V/s. Each curve represents an average of every probed cell at its particular temperature. It is clear from Fig. 5, that the overall trend of V_C (point of non-linearity) is to shift to higher values as the temperature decreases. At 5 volts per second, the amount of voltage required to induce electroporation increases by a factor of two (from 373 to 766 mV) as we lowered the temperature from 37 to 5°C. These findings are similar to those reported by Coster and Zimmermann in the membranes of *Valonia utricularis* cells [11]. This is a significant change considering that the membrane loses stability at transmembrane potentials exceeding 1 volt [2, 21, 22].
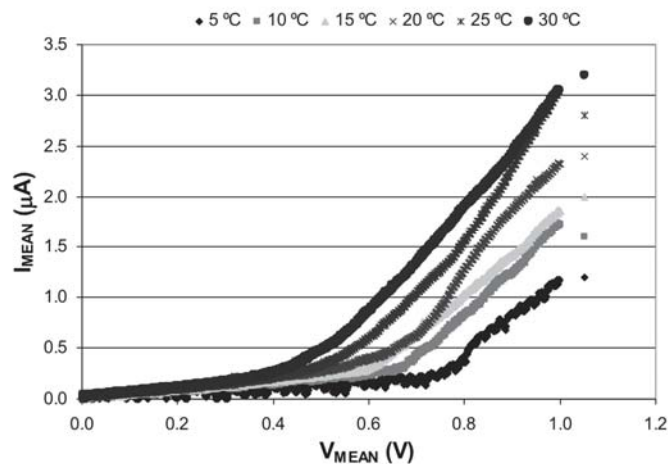
Fig. 5. Plot of average current vs. voltage for MDCK cells at different temperatures. The non-linearity observed in each curve is attributed to the electropermeabilization effect. The point of non-linearity is known as the critical voltage to induce electroporation (V_C). Notice that with increasing temperatures, V_C shifts to lower values.

3.3. Equivalent circuit results

The equivalent electrical circuit of the system can be used in conjunction with experimental data to determine the electrical variables of the circuit. In the curve of voltage versus current, (see Fig. 6A) where the slope represents the resistance

according to Ohm's law, the first segment of the curve is associated with the seal cleft resistance (see Figs. 3 A and 3C). This can be observed from Eq. 1 if it is considered that the membrane resistance is about three orders of magnitude larger than R_{seal} and R_{cyto} before electroporation starts (see [23]). Then, the equivalent resistance from Eq. 1 for the leftmost segment of Fig. **Error! Reference source not found.** takes the following form.

$$R_{Eq.} = R_{slope\ I} \approx R_{seal} \tag{2}$$

Therefore, the electrical recordings before electropermeabilization occurs pertain to the properties of the ionic solution of the seal cleft. Fig. 6B, shows the seal resistance as a function of temperature. As expected, the resistance increases monotonically with a temperature decrease (with the exception of the resistance at 25°C), typical of ionic solutions. However, the increase in ionic resistivity alone cannot account for the increase in resistance observed in Fig. 6B. This suggests that the seal cleft distance might change with temperature. The seal cleft distance was characterized, as a function of temperature, in an earlier study of ours and was attributed to the formation of a nano-channels between the cell membrane and the silicon nitride substrate [24].
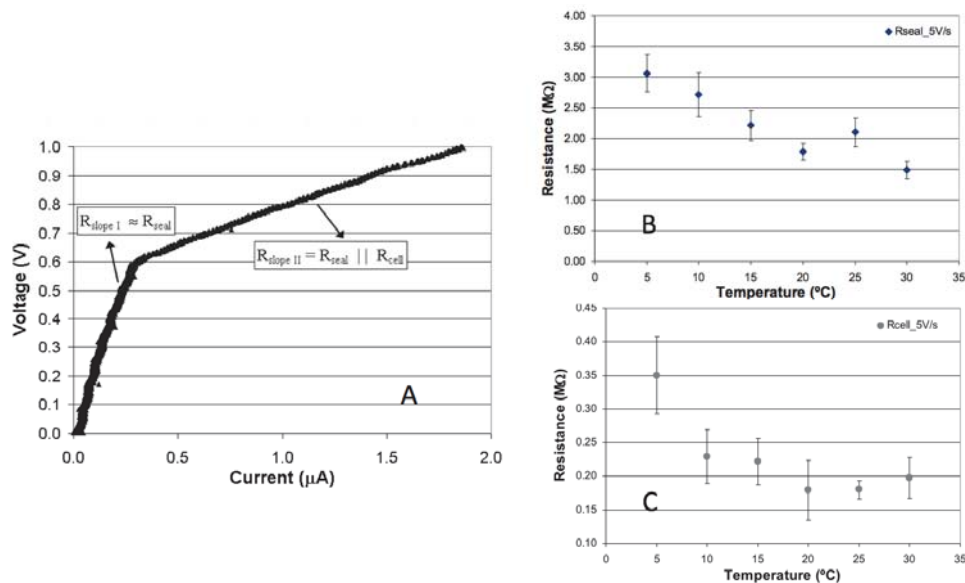
Fig. 6. A) Measured curve of voltage vs. current at the ramp rate of 5 V/s. B) Calculated seal resistance as a function of temperature for 5 V/s. The seal resistance is obtained from the slope of the first segment in the voltage vs. current graph C) Calculated cell resistance as a function of temperature during electroporation for 5 V/s. The error bars represent one standard deviation ($\pm\sigma$).

The second segment of the curve depicted on Fig. 6A represents the electrical recordings after electropermeabilization has occurred. Assuming that R_{seal} and R_{cyto} are constant during each pulse, the change in slope implies that the cell membrane

resistance has dropped drastically. This means that R_{cell} cannot be neglected anymore. Furthermore, we can estimate R_{cell} by employing the following equation:

$$R_{cell} = R_{seal}\left(\frac{R_{slope\,II}}{R_{slope\,I}-R_{slope\,II}}\right) \qquad (3)$$

where R_{slopeI} and $R_{slopeII}$ are the resistance values for the first and second segments respectively.

Fig 6 C, shows the temperature dependence of R_{cell} at the ramp rate of 5 V/s as estimated by employing the equation above. In general, this graph shows a weak temperature dependence on the cell resistance after electroporation has started. There is a notable change in resistance when the temperature reaches 5°C, but from 30 to 10°C the cell resistance is statistically close to a straight line. This observation becomes clear when the temperature dependence on R_{cell} is compared to that of R_{seal} and V_C. The temperature dependence of VC, is depicted in Fig. 7. The biophysical explanation of this behavior is not clear at first glance. However, this behavior could imply that the permeability state of the membrane stimulated by electric fields is less sensitive to temperature changes than the energy needed to induce electropermeabilization. This point can be better illustrated by normalizing the experimental data shown in Fig 5, with the V_C and I_C at each respective temperature (see Fig. 8). As it can be seen from Fig. 8, the normalized curves fall one on top of each other, suggesting a constant change in permeability regardless of temperature. This behavior has also been observed in planar lipid bilayers [25].

4. Discussion

The results of this study show that a key electroporation parameter, the critical voltage at the onset of electropermeabilization, V_C, is strongly dependent on temperature. This could be explained through the effect of temperature on the cell membrane. It has been established that several of the biophysical properties of the cell membrane change with temperature. These include: lipid phase transition [10], membrane elasticity [26] and membrane viscosity [27]. In this discussion, we will focus on the possible relationship between lipid-lipid interactions and the effect of temperature on V_C. The current versus voltage curves in Fig. 5 show that in addition to the actual value of the critical voltage, V_C, the pattern of the curve near the critical voltage also changes with temperature. At 30°C, the change in the slope of the curve is gradual while at 15°C, 10°C and 5°C the change in slope is much more abrupt. We suggest that the slope of the curves near the critical voltage may be related to the material properties of the cell membrane and their effect on the dynamics of the cell membrane permeabilization. The observed behavior may be associated to the behavior of polymeric materials in relation to their phase transition temperature (T_{PT}). Well above T_{PT} polymers behave as rubbery materials while well below T_{PT}, polymers behave as glassy materials [28]. In the range near T_{PT}, polymers behave as visco-elastic materials. Lipid membranes are also biological
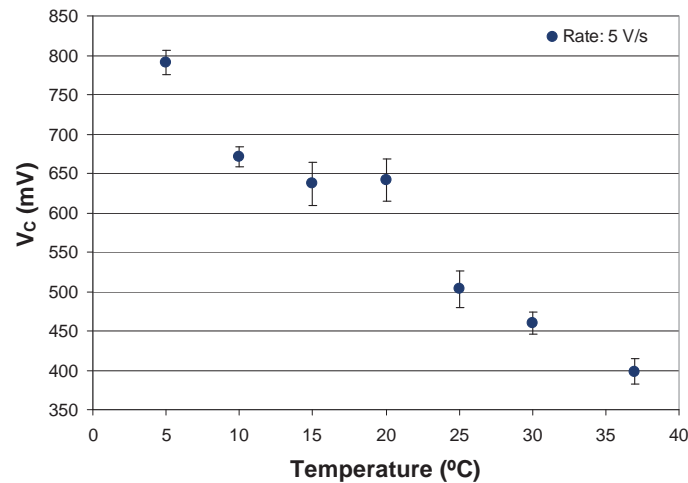
Fig. 7. Applied voltage at the onset of electroporation (V_C) as a function of temperature for a triangular waveform at 5 V/s. The error bars represent one standard deviation ($\pm 1\sigma$).

polymers that undergo thermotropic phase transition at a critical temperature, (T_{PT}). At this temperature the cell membrane changes upon cooling from a liquid-crystalline phase at physiological conditions to a lamellar gel phase [10, 29]. The liquid-crystalline state has fluid-like properties, as opposed to the highly organized structure of the gel phase [30]. The permeabilization of the cell membrane is a dynamic process related to a reorganization of the cell membrane in the presence of an electrical field. The change in slope with temperature observed in Fig. 5 could be explained through a change in the cell membrane elastic properties in relation to T_{PT}. The change in slope is abrupt (viscoelastic leaning towards gel) below this temperature range and gradual (viscoelastic leaning towards fluid) above this temperature range. The figure suggest that the phase transition temperature for MDCK cells is somewhere between 15°C and 20°C, to the resolution of our temperature measurement increment. No data on the lipid phase transition of MDCK cells was found in the literature to confirm the suggested value for this specific lipid phase transition temperature. However, roughly 70% of the phospholipid composition encountered in kidney mammalian cell membranes undergoes phase transition in temperatures ranging from 33°C to 14°C [29, 31].

The observation discussed above can provide valuable consideration in designing optimal electroporation protocols for cells in suspension. Most electroporation protocols are performed through the application of a constant electric field. Fig. 5 suggests that the electric potential needed to induce electroporation can be defined more precisely at lower temperatures, hypothetically below T_{PT}. This is because the range of values in which the transition from a normal state to an electroporated state, i.e. the critical voltage, is more defined at lower temperatures than at higher temperatures. At higher temperatures, the value of the critical voltage is less defined and a certain electroporation pulse in the

critical voltage range can have various effects on the permeabilization state of different cells within the population. In contrast, at lower temperatures there is a much sharper delineation between electrical parameters that induce electroporation and those that do not. Interestingly, similar results were found by Rols and colleagues [32]. They performed studies in which mammalian cells were electroporated at three different pre-incubation temperatures and the viability and transfection efficiency was evaluated. It was found that lowering the temperature from 37°C to 4°C before pulsation, produces a 10-fold increase in the transfection efficiency [32]. Our results may explain why.
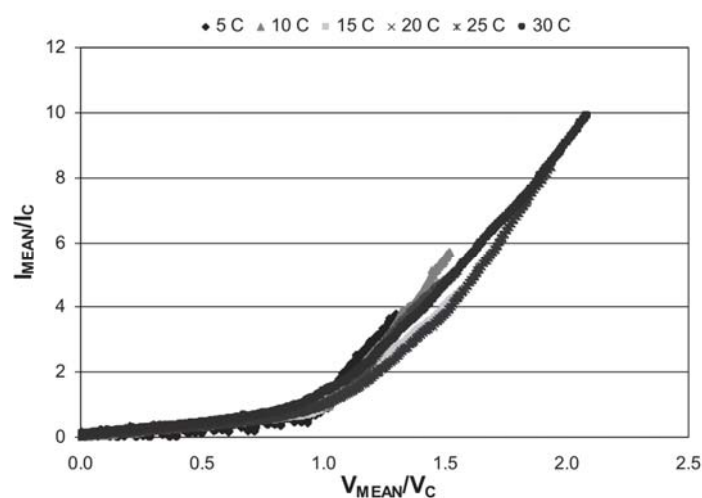
Fig. 8. Plot of normalized current vs. voltage for MDCK cells at different temperatures. Each data point has been normalized to their respective critical values for voltage or current. Notice that each curve falls on top of each other. Even though V_C changes strongly with temperature, the permeabilized state of the cell membrane seems to be temperature independent.

Even though the thermotropic phase transition of the lipid bilayer plays an important role on the temperature dependence of V_C, it alone cannot explain the behavior observed in Fig. 7. V_C appears to change continuously with temperature, throughout the analyzed temperature range, while the lipid phase transition should occur in a relatively narrower range. Therefore, it is likely that another biophysical mechanism may affect the electroporation behavior in addition to the lipid phase transition. This could be due to other cell membrane properties that vary with temperature like membrane elasticity and viscosity. It has been shown that both membrane elasticity and viscosity gradually increase with a decrease in temperature [26, 27]. This can be correlated to the results observed in Fig. 7. Experiments show that as the temperature is lowered, there is an increase in the membrane elasticity and viscosity, which is attributed to the increase in the strength of the lipid-to-lipid bond. The lipid-to-lipid bond strength increases with a decrease in temperature for two main reasons. First, there is less thermal energy

(kT) to break lipid bonds or contribute to the energy needed to break the bond among lipids. Second, the organized structure formed in the bilayer membrane due to the lipid phase transitions yields a stronger interaction among lipids. It is believed that electroporation causes a rearrangement of the lipids in the membrane. The discussion above suggests that there should also be an increase in the potential energy needed to induce electroporation as the temperature is lowered from physiological conditions due to the strengthening of the lipid-to-lipid bond. This is consistent with the results in Fig. 7.

Another interesting observation can be found in Fig. 8. The figure shows that the permeabilization state of the cell membrane after electroporation is independent on temperature. This suggests that once electroporation has occurred the cell membrane has taken a new stable configuration. Furthermore, the features in the cell membrane that correspond to a permeabilized state are dominant over the other mass transport features of the cell membrane. The experimental behavior we note has also been observed in planar lipid bilayers [25].

5. Conclusion

The goal of this study was to generate a better understanding of electroporation, the permeabilization of cell membranes through the application of electrical pulses. Studies show that there is a relationship between the process of electroporation and the properties of the cell membrane. Since temperature has an effect on membrane properties, the change in electrical parameters of electroporation with temperature were tested using a device capable of studying the electrical parameters of electroporation in individual cells. A series of experiments were performed with MDCK cells to determine the effect of temperature on electroporation. The results show a strong effect of temperature on electroporation parameters. It is found that the critical potential at the onset of electroporation, V_C, increases with decreasing temperature. Experimental results show that the critical voltage for electroporation at 5°C could be as much as two times the voltage needed to electroporate cells at 37°C. A possible explanation was proposed for this strong temperature dependence of V_C in relation to the lipid-lipid interactions within the cell membrane.

Furthermore, our results may explain why experiments show that lowering the temperature from 37°C to 4°C before pulsation, causes a 10-fold increase in the transfection efficiency as observed by others. From Fig. 5, it can be seen that the potential needed to induce electroporation appears to be more specific (narrower range of values) at temperatures below 15°C. Therefore, at temperatures below 15°C, a finer line can be drawn between electrical parameters that induce electroporation and those that do not when compared to results obtained at higher temperatures. This can potentially allow for better control of electroporation of cells in suspension.

An equivalent electrical circuit was developed to analyze the system. The equivalent electrical circuit analysis shows that the resistance imposed by the cell membrane during electropermeabilization had weak temperature dependence. The

same was true for the permeability state of the cells, even though V_C was found to be strongly temperature dependent.

References

[1] T.Y. Tsong, *Electroporation of Cell-Membranes*, Biophysical Journal, 60 (1991) 297-306.

[2] J.C. Weaver, *Electroporation of biological membranes from multicellular to nano scales, Dielectrics and Electrical Insulation, IEEE Transactions on* [see also Electrical Insulation, IEEE Transactions on], 10 (2003) 754-768.

[3] E. Neumann, A.E. Sowers, C.A. Jordan, *Electroporation and electrofusion in cell biology*, Plenum Press, New York, 1989.

[4] D.C. Chang, *Guide to electroporation and electrofusion*, Academic Press, San Diego, 1992.

[5] J. Gehl, *Electroporation: theory and methods, perspectives for drug delivery, gene therapy and research*, Acta Physiologica Scandinavica, 177 (2003) 437-447.

[6] J.C. Weaver, *Electroporation Theory*, in: J.A. Nickoloff (Ed.) Plant cell electroporation and electrofusion protocols, Humana Press, Totowa, N.J., 1995, pp. 3-28.

[7] F.J. Blatt, *Temperature dependence of the action potential in Nitella flexilis*, Biochimica et Biophysica Acta (BBA) - Biomembranes, 339 (1974) 382-389.

[8] S.A. Gallo, et al., *Temperature-Dependent Electrical and Ultrastructural Characterizations of Porcine Skin upon Electroporation*, Biophys. J., 82 (2002) 109-119.

[9] R. Hochmuth, K. Buxbaum, E. Evans, *Temperature dependence of the viscoelastic recovery of red cell membrane*, Biophys. J., 29 (1980) 177-182.

[10] P.J. Quinn, *A Lipid-Phase Separation Model of Low-Temperature Damage to Biological Membrane*, Cryobiology, 22 (1985) 128-146.

[11] H.G.L.a.U.Z. Coster, *The mechanism of electrical breakdown in the membranes of Valonia utricularis*, J. Membrane Biol., 22 (1975) 73-90.

[12] R. Benz, F. Beckers, U. Zimmermann, *Reversible Electrical Breakdown of Lipid Bilayer Membranes - Charge-Pulse Relaxation Study*, Journal of Membrane Biology, 48 (1979) 181-204.

[13] J. Kinosita, Kazuhiko, T.Y. Tsong, *Voltage-induced conductance in human erythrocyte membranes, Biochimica et Biophysica Acta (BBA) - Biomembranes*, 554 (1979) 479-497.

[14] S.A. Gallo, A. Sen, M.L. Hensen, S.W. Hui, *Temperature-Dependent Electrical and Ultrastructural Characterizations of Porcine Skin upon Electroporation*, Biophys. J., 82 (2002) 109-119.

[15] S.N. Murthy, A. Sen, Y. Zhao, S.W. Hui, *Temperature Influences the Postelectroporation Permeability State of the Skin*, Journal of Pharmaceutical Sciences, 93 (2004) 908-915.

[16] Y. Huang, B. Rubinsky, *Micro-electroporation: improving the efficiency and understanding of electrical permeabilization of cells*, Biomedical Microdevices, 2 (1999) 145-150.

[17] Y. Huang, B. Rubinsky, *Micro-electroporation: improving the efficiency and understanding of electrical permeabilization of cells*, Biomedical Microdevices|Biomedical Microdevices, 2 (1999) 145-150.

[18] Y. Huang, N.S. Sekhon, J. Borninski, N. Chen, B. Rubinsky, *Instantaneous, quantitative single-cell viability assessment by electrical evaluation of cell membrane integrity with microfabricated devices*, Sensors and Actuators a-Physical, 105 (2003) 31-39.

[19] A. Stett, V. Bucher, C. Burkhardt, U. Weber, W. Nisch, *Patch-clamping of primary cardiac cells with micro-openings in polyimide films*, Medical & Biological Engineering & Computing, 41 (2003) 233-240.

[20] R.E. Diaz-Rivera, B. Rubinsky, *Electrical and thermal characterization of nanochannels between a cell and a silicon based micro-pore*, Biomedical Microdevices, 8 (2006) 25-34.

[21] J.C. Weaver, Y.A. Chizmadzhev, *Theory of electroporation: A review, Bioelectrochemistry and Bioenergetics*, 41 (1996) 135-160.

[22] J.C.a.Y.A.C. Weaver, *Theory of electroporation: A review, Bioelectrochemistry and Bioenergetics*, 41 (1996) 135-160.

[23] B. Sakmann, E. Neher, *Single-channel recording*, Plenum Press, New York, 1983.

[24] R.E. Diaz, *Micro and Nano Scale Bioelectronics in Cell Micro-electroporation*, Department of Mechanical Engineering, University of California, Berkeley, Fall 2005, Berkeley, 2005.

[25] R. Basu, et al., *Nonlinear conduction in bilayer lipid membranes - effect of temperature*, Physica A: Statistical Mechanics and its Applications, 292 (2001) 146-152.

[26] R. Dimova, B. Pouligny, C. Dietrich, *Pretransitional effects in dimyristoylphosphatidylcholine vesicle membranes: Optical dynamometry study*, Biophysical Journal, 79 (2000) 340-356.

[27] A.J. Wang, K.S. Hu, *Calibration of membrane viscosity of the reconstituted vesicles by measurements of the rotational diffusion of bacteriorhodopsin*, Chin. Phys. Lett., 19 (2002) 1727-1729.

[28] N.G. McCrum, C.P. Buckley, C.B. Bucknall, *Principles of polymer engineering*, 2nd ed. ed., Oxford University Press, Oxford ; New York, 1997.

[29] J.R. Silvius, *Thermotropic phase transition of pure lipids in model membranes and their modification by membrane proteins*, in: P.C. Jost, O.H. Griffith (Eds.) Lipid-protein interactions, Wiley, New York, 1982, pp. 240-276.

[30] M.N. Jones, D. Chapman, *Micelles, monolayers, and biomembranes*, Wiley-Liss, New York, 1995.

[31] D. White, *The phospholipid composition of mammalian tissues*, in: P.C. Jost, O.H. Griffith (Eds.) Lipid-protein interactions, Wiley, New York, 1982, pp. 441-482.

[32] M.P. Rols, C. Delteil, G. Serin, J. Teissie, *Temperature Effects on Electrotransfection of Mammalian-Cells*, Nucleic Acids Research, 22 (1994) 540-540.